Transport and Accretion Processes in Protoplanetary Disks: A New Paradigm

Xue-Ning Bai

Email: xbai@cfa.harvard.edu

**Institute for Theory and Computation,
Harvard-Smithsonian Center for Astrophysics,
60 Garden St., MS-51, Cambridge, MA, 02138**

Introduction: Protoplanetary disks (PPDs) are widely believed to be turbulent as a result of the magnetorotational instability (MRI). However, the properties of the MRI strongly depend on non-ideal magnetohydrodynamic (MHD) effects including Ohmic, Hall and ambipolar diffusion due to the weakly ionized nature of PPDs. Conventional picture of layered accretion considers only the effect of Ohmic resistivity. We perform local 3D MHD simulations of PPDs that for the first time, take into account both Ohmic resistivity and ambipolar diffusion (AD) in a self-consistent manner. We show that the inner disk (<10 AU) is largely laminar with the MRI suppressed and wind-driven accretion. The outer disk is likely to be MRI turbulent with weak outflow.

Method and simulations: We use the Athena MHD code, and conduct 3D stratified local shearing-box simulations. Ohmic and ambipolar diffusivities are obtained self-consistently in real simulation time from a pre-computed a look-up table based on equilibrium chemistry using a complex chemical reaction network (see Bai, 2011) assuming well-mixed 0.1μm grains with abundance of 10^{-4}. Note that Ohmic resistivity dominates in the midplane region of the inner disk (<10 AU), while AD dominates in low-density regions (inner disk upper layer and outer disk). Most of our simulations include net vertical magnetic flux characte-rized by β_0, ratio of gas to magnetic pressure (of the net vertical field) at midplane. We adopt the MMSN disk model and isothermal equation of state. Velocity and length are measured in sound speed c_s and scale height $H=c_s/\Omega$.

Fiducially, we fix our calculations at 1 AU with $\beta_0=10^5$. The simulation box is illustrated in the right panel, where the three dimensions are radial (x), azimuthal (y) and vertical (z), and the box size is ($4H\times8H\times16H$). For all our simulations, the initial field configuration is unstable to the MRI in the disk upper layer ($z\sim3H$). Shown on the right is a snapshot of the initial development of the MRI at 2 orbits. The volume rendering shows gas density, increasing from blue to red at midplane. The streamlines indicate the gas velocity, increasing from blue (v=0) to red (v=5).

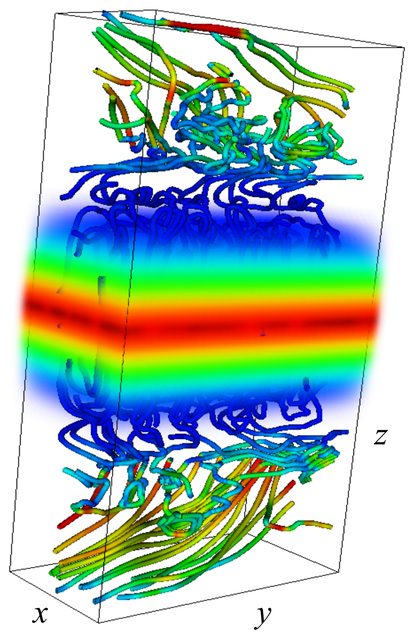

1. MRI suppression and Wind Launching

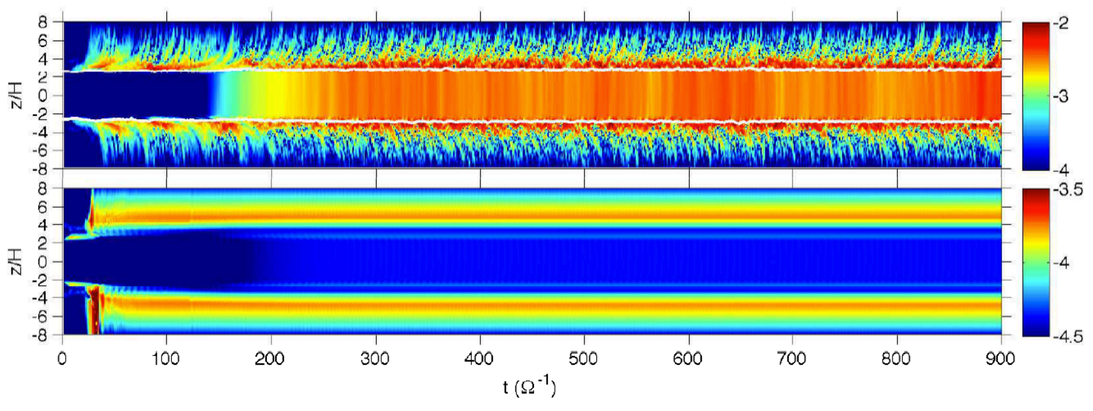

To demonstrate the dramatic role of AD, we perform two contrasting simulations with exactly the same initial conditions. The first (top) included only the Ohmic resistivity, while the second (bottom) included both Ohmic resistivity and AD. The above figure is the space-time plot of horizontally averaged vertical profiles of Maxwell stress [log($-B_xB_y$)]. The top panel simply illustrates the conventional picture of layered accretion, with active MRI turbulence beyond z~±2H. When AD is included, even the initial condition is unstable to the MRI (i.e., the previous figure), the system quickly relaxes to a laminar state: the MRI is completely suppressed. This is because AD is the dominant effect at disk upper layer, where weak magnetic field is essential for MRI to operate (Bai & Stone, 2011). The initial magnetic field is over-amplified by the transient MRI, leading to self-quenching. This process is very robust, independent of initial conditions.

2. Wind Structure

The laminar state in fact corresponds to a magneto-centrifugal driven disk wind. The right figure illustrates the geometry of the poloidal magnetic field line (blue) & velocity vectors (red). The midplane region (≤2H) is magnetically decoupled due to excessively large resistivity. The wind is launched from a vertical gradient of toroidal magnetic field (mostly around 2~4.5H), leading to outward drift of ions, which bends the magnetic field. When sufficient bending angle (>30°) is achieved, the outflowing gas is centrifugally accelerated along open magnetic field lines (Blandford & Payne, 1982).

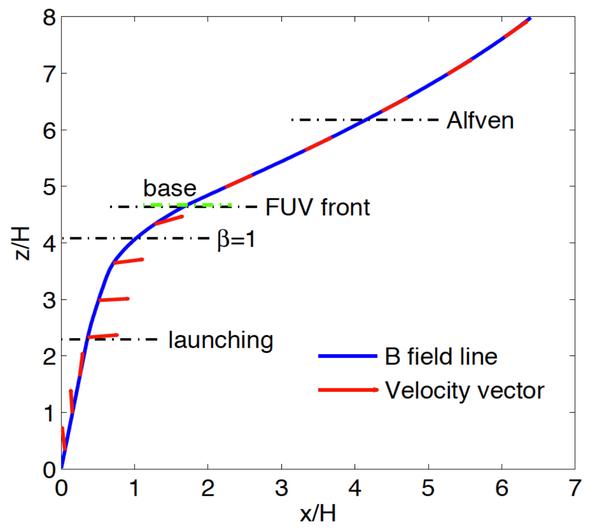

3. Wind-driven accretion and Wind Symmetry

The shearing-box model does not distinguish radial directions. Correspondingly, the wind has two possible geometries shown on the right. The left case is unphysical since the outflows at the top and bottom point to opposite radial (x) directions. The right case is physical, with an additional "kink" feature at $z\sim3H$.

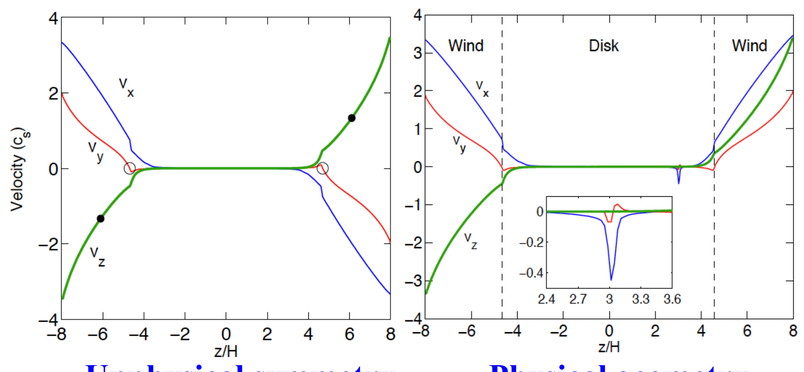

The location of the kink corresponds to where the horizontal magnetic field flips (i.e., a strong current layer). Note that it is offset from the magnetically decoupled midplane. The gas drifts inward very rapidly (approaches the sound speed) at the strong current layer. In fact, this strong current layer carries the entire accretion flow. With a weak net flux of $\beta_0=10^5$, we find that accretion rate of $5\times10^{-8}M_\odot\mathrm{yr}^{-1}$ can be easily achieved (at 1AU).

4. Radial Dependence and Global Picture of PPDs

We have extended our calculations to larger disk radii up to 15 AU, from which we have obtained criteria for launching the laminar disk wind as follows:

1. Ohmic resistivity dominated midplane (true at inner disk).
2. AD dominated disk surface (always holds).
3. Presence of weak net vertical magnetic field (very likely).
4. Gas coupled to magnetic field at wind zone (true by far UV ionization, etc.).

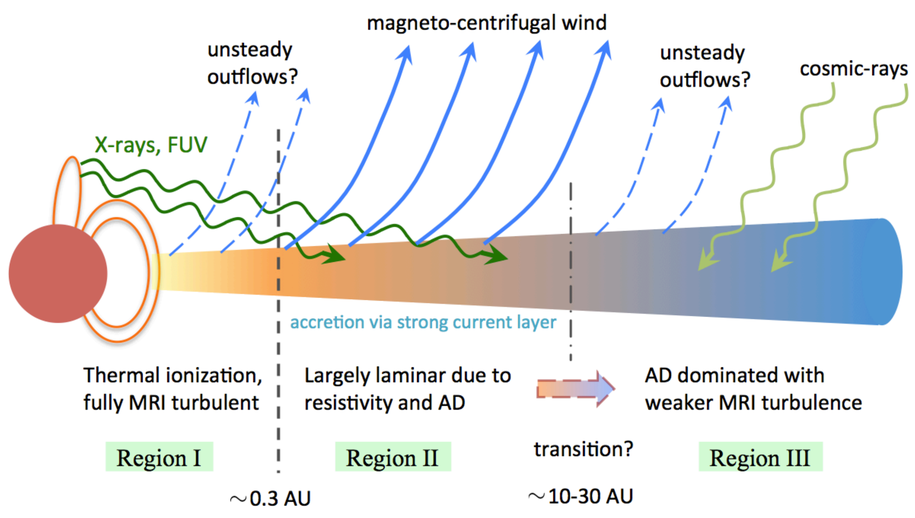

Based on our simulations, a new paradigm for the accretion process in PPDs emerges as illustrated in the Figure above. The innermost region of the PPD is not subject to non-ideal MHD effects due to thermal ionization. At intermediate radii (~0.3-10 AU), the disk is largely laminar, launching a strong magnetocentrifugal wind which efficiently drives disk accretion. We have obtained a fitting formula for wind-driven accretion rate:

$$\dot{M}\approx0.91\times10^{-8}M_\odot\ \mathrm{yr}^{-1}\ R_{\mathrm{AU}}^{1.21}\left(\frac{B_{z0}}{10\ \mathrm{mG}}\right)^{0.93},$$

where B_{z0} is the strength of the net vertical field threading the disk.

Beyond ~10 AU, MRI gradually sets in and becomes the dominant mechanism to drive accretion at the outer disk, mediated by strong AD (e.g., Simon, Bai, et. al. 2013).

Main References:

1. Bai, X.-N., Stone, J. M., "Wind-driven accretion in protoplanetary disks: I. Suppression of the MRI and launching of the magnetocentrifugal wind", 2013, ApJ, 769, 76

2. Bai, X.-N., "Wind-driven accretion in protoplanetary disks: II. Radial dependence and Global Picture", 2013, ApJ, 772, 96